621.436.016

Paper No. 214-13

Development and Use of a Spray Combustion Modeling to Predict Diesel Engine Efficiency and Pollutant Emissions*

(Part 2 Computational Procedure and Parametric Study)

by

Hiroyuki HIROYASU**, Toshikazu KADOTA***

and Masataka ARAI***

An algorithm for predicting heat release rate and pollutant emission in direct injection diesel engine has been developed according to the mathematical model mentioned in the first report.

Predictions made with the simulation have been compared with the data on a single-cylinder engine over a range of engine speeds, injection timings and swirl ratios. Predicted pressure diagram, and NO and soot emissions showed acceptable quantitative agreement with the data. A parametric study of the effect of variations in load, speed, injection rate, injection timing, swirl ratio and droplet size is then carried out.

1. Introduction

In the first report, a multi-zone model of diesel spray was developed for studies of the effect of variations on performance, efficiency and pollutant emissions. This model consists of two major portions, the heat release model and the emission formation model. The calculation of the concentration of emission (NO, soot and others) requires knowledge of temperature and equivalence ratio which depend upon space and time in the combustion chamber, and also cylinder pressure. The reason for this is that species such as NO and soot are formed in a nonequilibrium manner and their exhaust concentrations cannot be calculated solely from a knowledge of over-all equivalence ratio, exhaust temperature distribution and pressure. In order to determine pressure and temperature histories, and the local equivalence ratio, it is necessary to understand the detail mechanism of spray burning. The rate of spray burning determines the rate of energy release in the combustion chamber. Together with the piston motion, the heat release rate determines the pressure, temperature, and equivalence ratio variations in the cylinder, which in turn govern the chemical kinetics. The heat release model includes fuel injection simulation, spray formation, evaporation, ignition and heat release. The emission formation model includes the calculations of the chemical kinetics of equilibrium components, and NO and soot emissions. In the present study, an algorithm for predicting engine performance and exhaust emissions has been developed. Predictions made with the simulation have been compared with the data on a single-cylinder engine. Further, a parametric research of the effect of variations in load, speed, injection timing, etc., has been carried out.

2. Calculating Procedure and Results

Flow diagram for computation is illustrated in Fig. 1 for any arbitrary

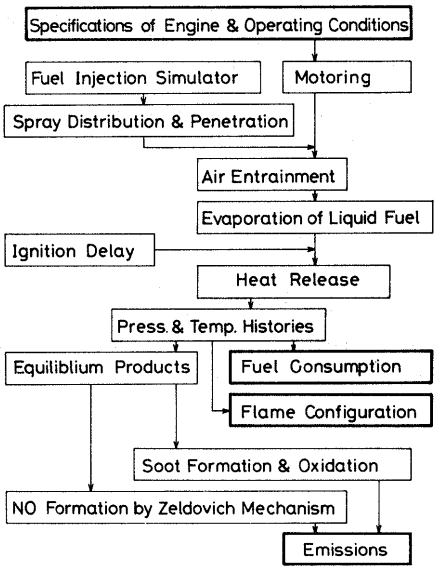

Fig. 1 Flow diagram for calculation

* Received 6th April, 1981.

** Professor, Faculty of Engineering, University of Hiroshima, Higashi-Hiroshima, Japan.

*** Associate Professor, Faculty of Engineering, University of Hiroshima, Higashi-Hiroshima, Japan

Table 1 Details of the direct-injection engine used in the experiment

Bore	0.135 m
Stroke	0.13 m
Length of Connecting Rod	0.23 m
Clearance Volume	0.1283×10^{-3} m^3
Swept Volume	1.8×10^{-3} m^3
Compression Ratio	15.0
Closing Timing of Inlet Valve	145 deg. BTDC
Opening Timing of Exhaust Valve	145 deg. ATDC
Injection Pump	Bosch AD
Plunger Bore	10 mm
Diameter of Nozzle Hole	0.35 mm
Number of Nozzle Holes	4

package. Spray is divided into 250 packages to all of which the method mentioned in the first report is adopted. Small increment of crank angle $\Delta\theta$ is 1°CA. Computation is made from the inlet valve closing (145°CA BTDC) to the exhaust valve opening (145°CA ATDC). To save the computation time, pollutant emissions are computed for only 18 packages according to these temperatures, pressures and equivalence ratios. These packages are picked up as typical packages such as the packages on the spray axis or in the periphery of the spray. The computation time for one engine operating condition is about 4 minutes using the computer of HITAC M-180. Details of the direct injection engine used in the experiment and simulating computation are shown in Table 1. The physical properties of the used fuel are those of n-dodecane. The ignition delay is assumed to be an ignition delay of the fuel with cetane number 60. Calculation is executed for each package according to the algorithm derived from the equations mentioned in the first report. Differential equations are solved by Runge-Kutta-Gill method and simultaneous equations are solved by an iteration method.

Fig. 2 represents a historical diagram of temperature in the packages. L in the figure represents the radial distance. L=1 and L=10 show central portion and peripheral portion of a spray respectively. I coincides with the order of injection. I=1 shows the tip portion of spray. J represents the ignition timing of the packages. Variations in NO concentration with the time in several packages are illustrated in Fig. 3. Concentration of NO increases with the lapse of time and reaches a peak value and thereafter decreases slightly and converges to a quenched value. The concentration of NO in the package of L=5, I=20 is low because of its low temperature history. NO concentration in the packages (L=10, I=10; L=1, I=1) which have burned in the early stage is high. Fig. 4 also shows the variation of soot concentration in the package. The soot formation level in the core of the spray is higher than on the periphery of the spray. When the fuel is consumed, the soot formation stops and only the soot oxidation continues. Fig. 5 is a historical diagram of the rate of heat release, the cylinder pressure and

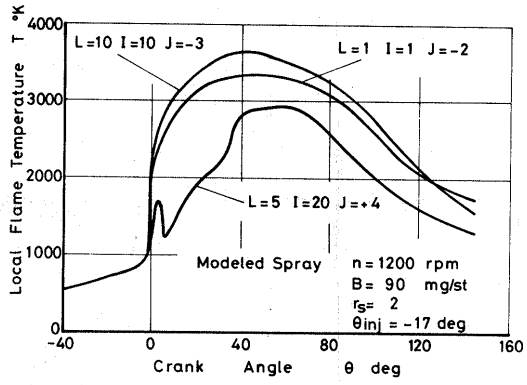

Fig. 2 Flame temperature history in the packages

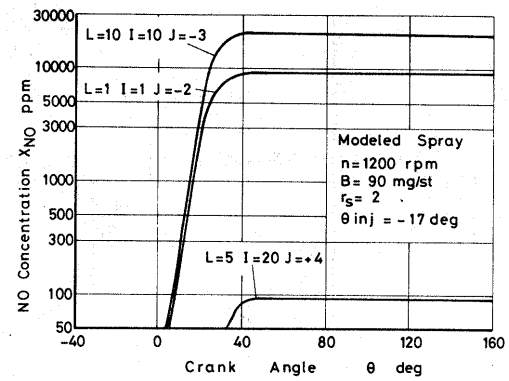

Fig. 3 NO concentration history in the packages

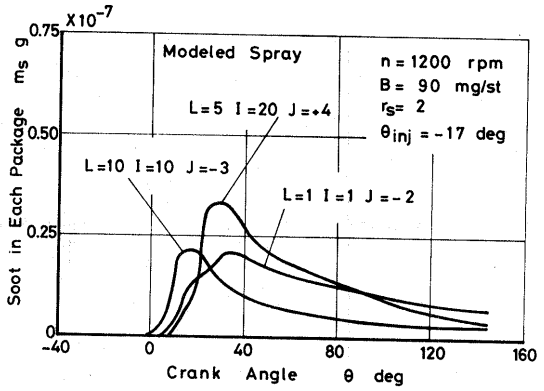

Fig. 4 Soot concentration history in the packages

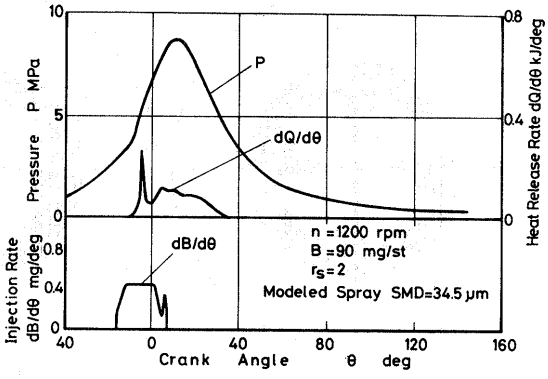

Fig. 5 Calculated injection rate, heat release and cylinder pressure

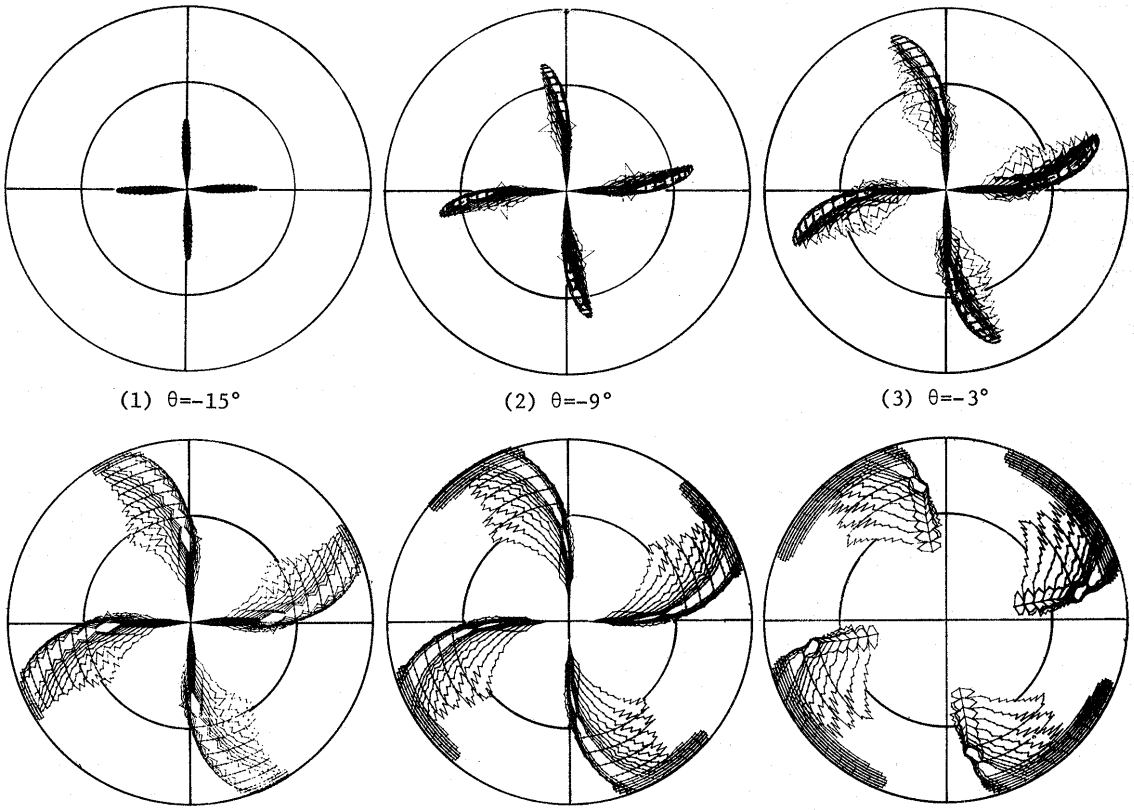

Fig. 6 Calculated spray and flame configuration impinging on the cylinder wall

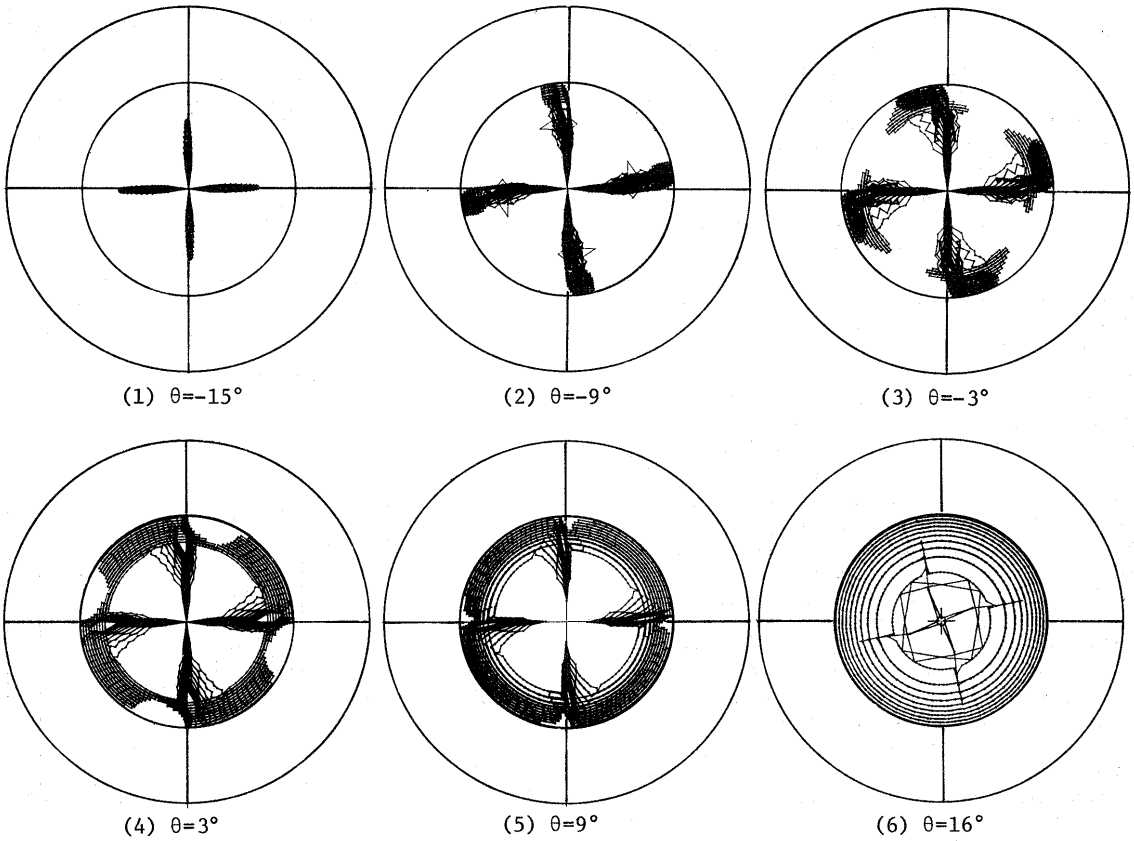

Fig. 7 Calculated spray and flame configuration impinging on the piston cavity

the injection rate.

Figs. 6 and 7 represent the fuel spray and the flame configuration calculated by the theoretical analysis. The shadow portions in the configuration show the packages which are not yet ignited and the others show the flame configuration, that is, the packages which are already ignited. The calculated spray and flame configurations impinging on the cylinder wall are shown in Fig. 6. In this case, the effect of swirl on the deformation of the configurations is very clear. Figure 7 shows the spray and flame configuration impinging on the piston cavity. In this case, the spray is assumed to burn out in a shallow dish bowl on the piston. In both cases, the packages on the periphery of the spray have smaller droplet and higher gas temperature than the center portions of the spray. Therefore ignition occurs first in these packages. After ignition occurs, a sudden expansion of the package and a temperature increase cause subsequent fuel evaporation and air entrainment. Therefore the remained fuel in the ignited package continues burning. It also causes a temperature increase which is entrained into the neighboring non-ignited package. Then the packages which surround the ignited package are easy to self-ignite. In other words, the number of ignited packages increases rapidly. It is as if the combustion flame propagates in the spray.

A 4-holes injection nozzle is used under this calculating condition, but the configuration is calculated for only a single spray by assuming non-interference of sprays. The amount of injected fuel and charged air which is consumed for combustion of four sprays is also divided into four groups. Both Figs. 6 and 7 are drawn automatically by an X-Y plotter of HITAC M-180.

3. Comparison of Computed Predictions with Experimental Results

In order to confirm the availability of the simulation results for the prediction of engine performance and pollutant emissions, simulation results are compared with experimental results.

A four-cycle, single-cylinder, water-cooled, direct-injection diesel engine (Mitsubishi DT-6) as shown in Table 1 was utilized in the experiment, of which combustion chamber was of a shallow toroidal type. The bore and the stroke of the engine were 135mm and 130mm respectively. Compression ratio was 15.0. Injection pump used was Bosch AP with a plunger diameter 10mm. A long injection nozzle with 4 holes (DLL-160S354, Diesel-kiki) was used. The injection angle and opening pressure of the nozzle was 160deg. and 2.2MPa.

Cylinder pressure was measured with a piezo electric pressure pickup (12QP300, AVL), of which output was recorded with an oscilloscope. The needle lift of the injection nozzle was detected with a light beam chopping-type detector. Apparatus for measuring NO in the exhaust was of chemiluminescence type (ECL-7_S, Yanagimoto). Soot was measured at a mixing chamber which was used as an exhaust silencer by a Bosch Smoke Meter. Soot concentration was derived from Bosch Smoke Number by multiplying a exchanging coefficient.

Figure 8 represents the pressure histories in the combustion cylinder at various injection timings. The calculated results presented in solid lines were compared with the experimental results as shown in dotted lines. Both results of the pressure histories have the same dependence upon the injection timing. Earlier injection resulted in a higher peak pressure. Figure 9 shows the effect of the injection timing on the concentration of nitric oxide and smoke in the exhaust gas.

The formations of combustion products ware calculated within each element of spray with equilibrium or non-equilibrium manner and they were integrated over the entire spray, which gave the concentration of chemical species in the exhaust gas. NO and soot were calculated in a non-equilibrium manner. The calculated value of exhaust NO is lower than the experimental one. One reason is that the calculated flame temperature is fairly lower than the expected one. But it shows

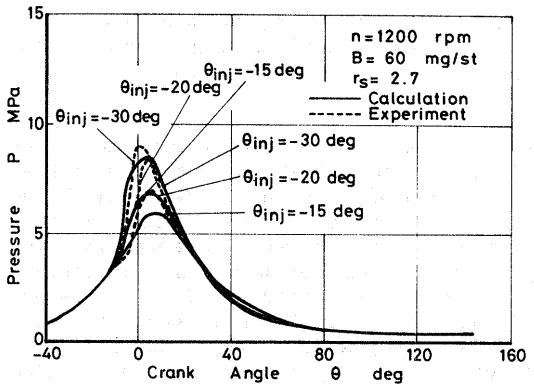

Fig. 8 Effect of injection timing on calculated and experimental cylinder pressure

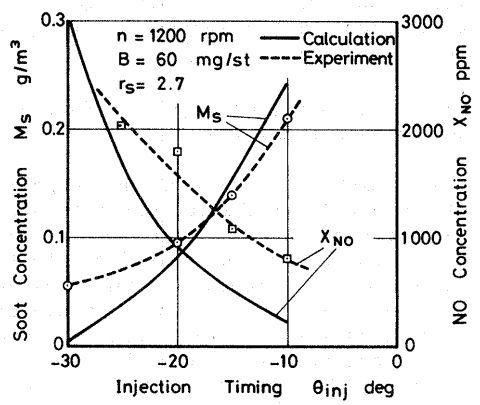

Fig. 9 Effect of injection timing on calculated and experimental soot and NO concentration

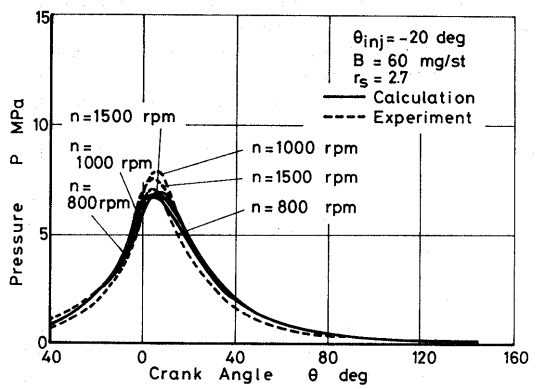

Fig. 10 Effect of engine speed on calculated and experimental cylinder pressure

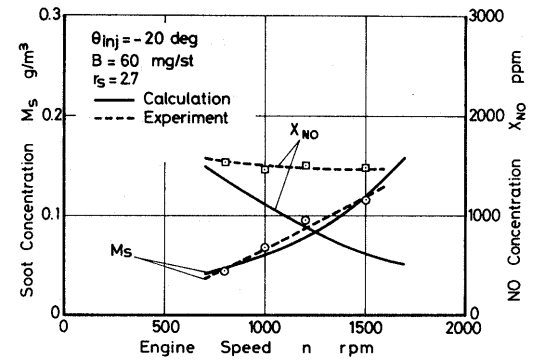

Fig. 11 Effect of engine speed on calculated and experimental soot and NO concentration

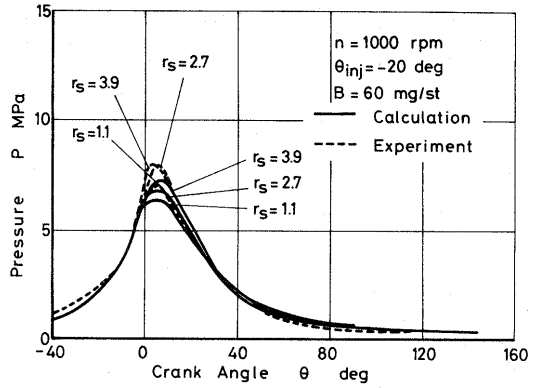

Fig. 12 Effect of swirl ratio on calculated and experimental cylinder pressure

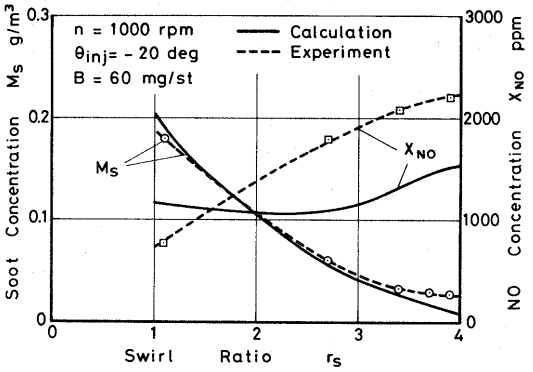

Fig. 13 Effect of swirl ratio on calculated and experimental soot and NO concentration

that these results are useful for predicting trends of NO concentration rather than absolute values. Calculated NO concentration decreases and soot concentration increases with a retarding injection. Figure 10 shows the theoretical and experimental results of the pressure history in the cylinder at various engine speeds. Figure 11 shows NO and soot concentration dependence upon the engine speed. NO decreases but soot increases with an increasing engine speed. Figures 12 and 13 show the effects of air swirl on the cylinder pressure, soot and NO concentration. The experimental data shown in these figures were obtained by using a shrouded valve engine.

4. Parametric Study of Engine Performance and Pollutant Emissions

The similarity between the experimental pressure and theoretical pressure, and good prediction of the effect of many parameters on NO and soot emissions, imply that the model developed in the present paper is regarded as a potentially useful tool for predicting the heat release rate and the concentrations of the exhaust emissions. Parametric studies were therefore attempted. In the calculation of the parametric studies, papameters were changed one by one. For example, droplet mean size was changed with spray penetration, injection rate, etc., unchanged which are variable with droplet mean size in a practical engine.

4.1. Effect of injection timing

Figures 14 and 15 show the effect of the injection timing on cylinder pressure, heat release rate, soot, NO concentration and specific fuel consumption. In this computation, the droplet size, injection rate, swirl ratio, etc. were kept constant and only the injection timing was changed. Advanced injection timing leads to increases in the temperature and in NO concentration, and a decrease in the soot concentration.

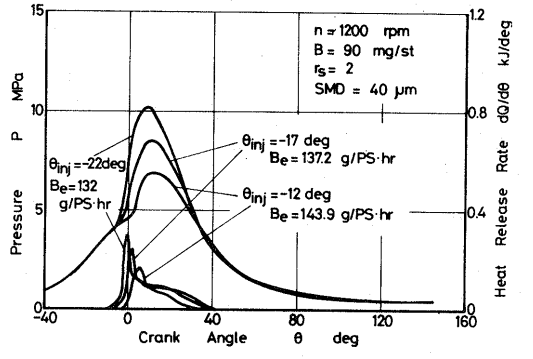

Fig. 14 Effect of injection timing on pressure and heat release

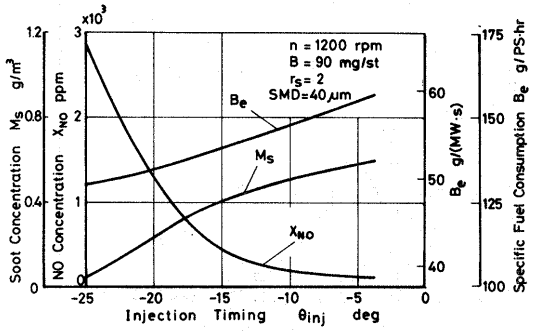

Fig. 15 Effect of injection timing on emissions and fuel consumption

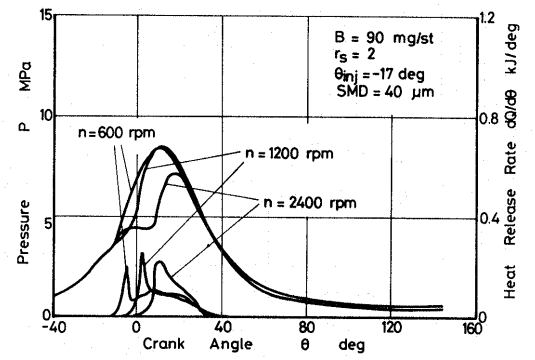

Fig. 16 Effect of engine speed on pressure and heat release

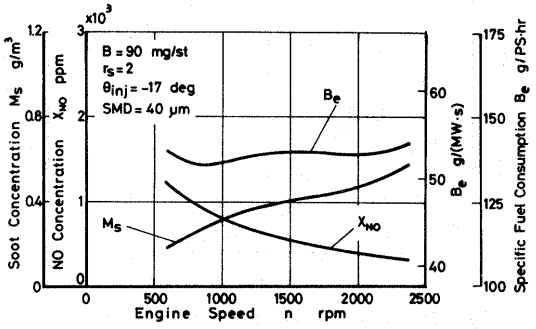

Fig. 17 Effect of engine speed on emissions and fuel consumption

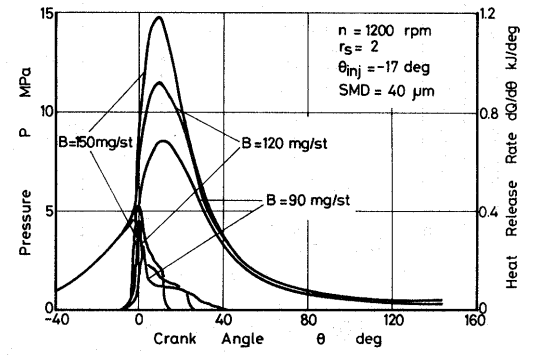

Fig. 18 Effect of amount of fuel on pressure and heat release

4.2. Effect of engine speed

Figures 16 and 17 represent the effect of the engine speed on engine performances and emissions. These results were obtained by keeping injection timing, injection rate, etc., constant. NO concentration decreased with an increasing engine speed. This is presumably due to the decrease in the period of time for reaction and to the suppression of increasing cylinder pressure and temperature. On the other hand, soot concentration increased with an increasing engine speed because soot was slowly oxidized with air, and reaction time decreased with an increasing engine speed.

4.3. Effect of fuel amount

Effects of amount of fuel on cylinder pressure and heat release rate are shown in Fig. 18. The effect of the quantity of fuel injected on NO and soot concentration in the exhaust gas and specific fuel consumption is shown in Fig. 19. Since the injection period was constant for all conditions, the quantity of fuel injected was controlled by the rate of fuel injection. In general, if the quantity of injected fuel is changed, the mean droplet size of spray and spray tip penetration would be changed. However, in this computation, the droplet size was kept constant, for example 40μm and the spray tip penetration and the air entrainment to the spray were changed. The amount NO and soot increase with an increasing amount of injected fuel. But specific fuel consumption rate once has the minimum value.

4.4. Effect of swirl ratio

Figures 20 and 21 show the effect of swirl ratio on engine performance and emissions. Since the non-overlapping of the spray at high swirl ratio is assumed, an increasing swirl ratio leads to a higher rate of droplet evaporation and an increase in the air entrainment. Consequently, this results in the higher cylinder pressure and NO concentration. It is also seen that the soot concentration and specific fuel consumption decrease with an increasing velocity of swirling air. This is due to the fact that the soot oxidation increases with air.

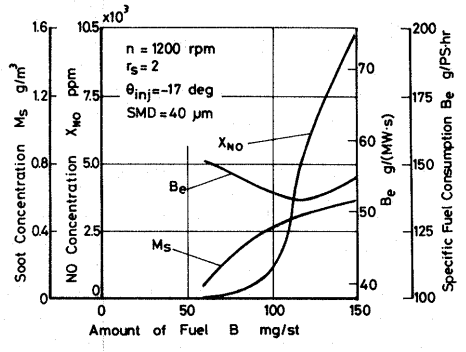

Fig. 19 Effect of amount of fuel on emissions and fuel consumption

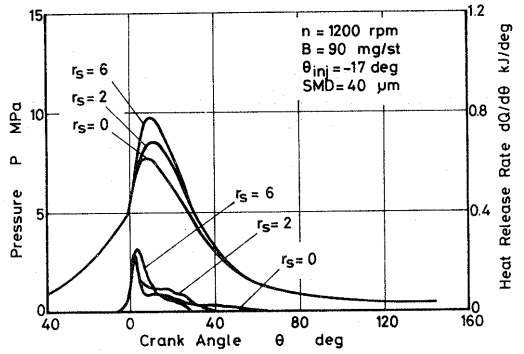

Fig. 20 Effect of swirl ratio on pressure and heat release

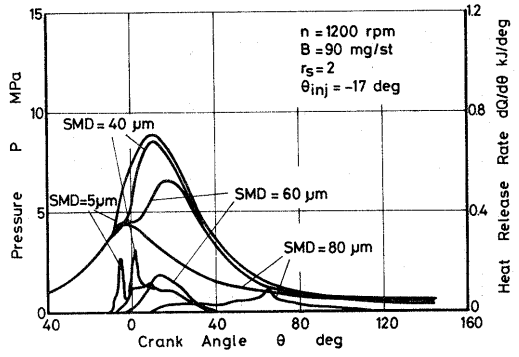

Fig. 22 Effect of mean droplet size on pressure and heat release

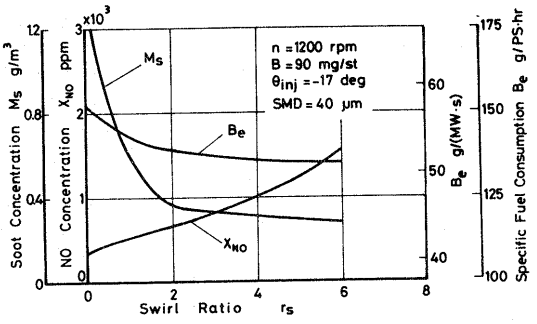

Fig. 21 Effect of swirl ratio on emissions and fuel consumption

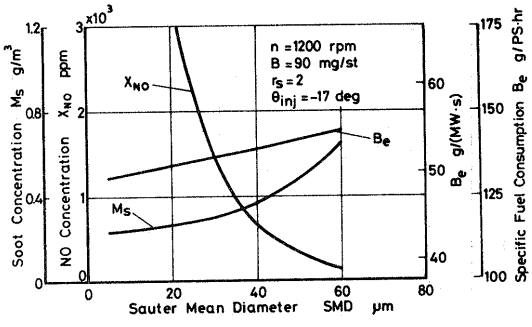

Fig. 23 Effect of mean droplet size on emissions and fuel consumption

4.5. Effect of droplet size

The effect of Sauter mean diameter in sprayed droplet on engine performance and emissions is shown in Figs. 22 and 23. When the mean droplet diameter is larger than 40μm, the evaporation rate of droplets is slow, and the heat release rate is greatly affected by the evaporation rate. On the other hand, when the mean diameter is smaller than 40μm, the evaporation rate does not greatly affect the combustion phenomenon. However, an increasing mean droplet size leads to a decrease in NO concentration and an increase in soot concentration.

4.6. Effect of injection pressure

Figures 24 and 25 show the effect of variations in injection pressure under constant injected fuel amount and under the selected diameter of injection nozzle holes. When the amount of injected fuel is constant, a smaller nozzle hole means a higher injection pressure. Soot concentration and specific fuel consumption decrease and NO concentration increases with an increasing injection pressure.

4.7. Effect of injection rate

Figure 26 shows the effect of injection rate on the cylinder pressure and heat release rate. Shown in Fig. 27 is NO and soot concentration and specific fuel consumption affected by the rate diagram of the fuel injection, where the quantity of fuel injected, injection timing, and injection period are kept constant. When a large quantity of fuel is injected

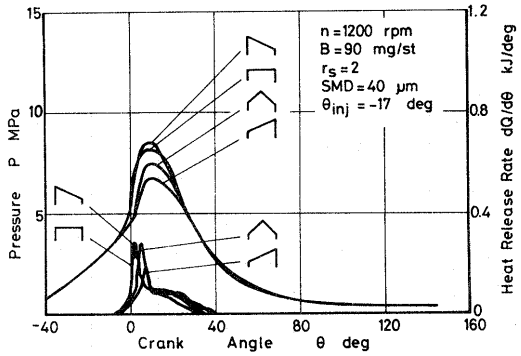

Fig. 24 Effect of the pattern of injection rate on pressure and heat release

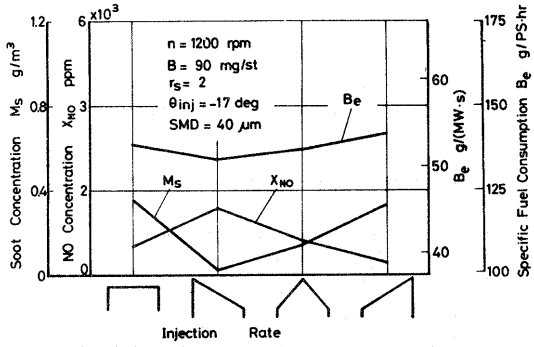

Fig. 25 Effect of the pattern of injection rate on emissions and fuel consumption

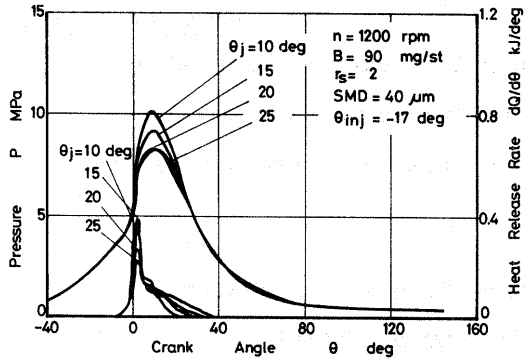

Fig. 26 Effect of injection duration on pressure and heat release

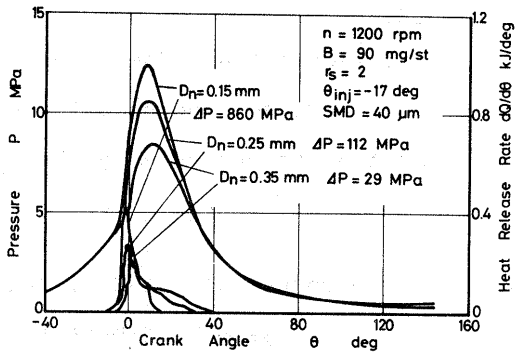

Fig. 28 Effect of injection pressure on pressure and heat release

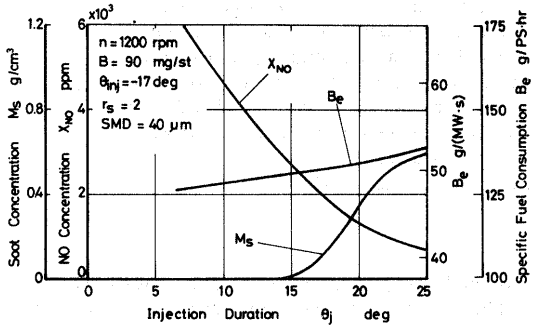

Fig. 27 Effect of injection duration on emission and fuel consumption

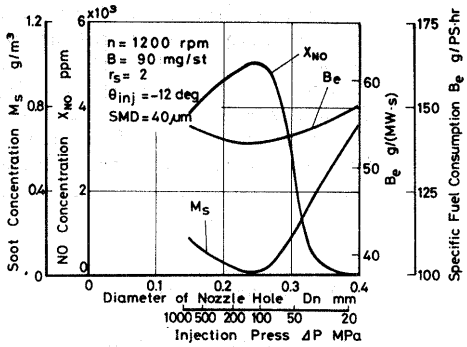

Fig. 29 Effect of injection pressure on emissions and fuel consumption

during the early part of injection, high NO concentration and low soot concentration are obtained. The results are different when the fuel is mostly injected during the last part of injection.

4.8. Effect of injection pressure

Figures 28 and 29 show the effect of injection pressure on the engine performance and emissions. When the amount of injected fuel is constant, a shorter injection duration means a higher injection pressure. Soot concentration and specific fuel consumption increase and NO concentration decreases with an increasing injection duration.

5. Conclusions

A mathematical model for predicting heat release rate and emission concentration in diesel engines was used. In the model, emphasis was placed on the detailed physical processes in the combustion chamber and on the employment of a minimum of necessary approximations. The validity of this model was examined by comparing predictions made with simulation of data on a direct injection single-cylinder engine over a range of injection timings, engine speeds, fuel amounts and swirling ratios. Predicted engine performance and pollutant emissions showed acceptable quantitative agreement with the data.

A parametric study on the effects of variations in injection timing, engine speed, fuel amount, swirl ratio, droplet size, injection pressure, and injection rate was completed.

Acknowledgement

The authors wish to thank the financial support of Grant-in-Aid Scientific Research from the Ministry of Education, Japan.